PROTON STRUCTURE FROM HIGH ENERGY PROTON-PROTON AND ANTIPROTON-PROTON ELASTIC SCATTERING

M. M. Islam[1], J. Kašpar[2,3], R. J. Luddy[1]
[1]Department of Physics, University of Connecticut, Storrs, CT 06269 USA
[2]Institute of Physics of the Academy of Sciences of the Czech Republic, Prague, Czech Republic
[3]CERN 1211 Geneva 23, Switzerland

Abstract

Our phenomenological investigation of high energy pp and p̄p elastic scattering and study of the gauged Gell-Mann-Levy linear σ-model using path-integral formalism have led us to a physical picture of the proton structure. Namely, proton is a **Condensate Enclosed Chiral Bag**. Based on this picture, our prediction of pp elastic scattering at c.m. energy 7 TeV is discussed against the backdrop of recent measurements of elastic pp $d\sigma/dt$ at LHC by the TOTEM Collaboration at $\sqrt{s} = 7$ TeV.

1. Introduction

High energy pp and p̄p elastic scattering have been at the forefront of particle physics research since the early seventies with the advent of the CERN ISR pp collider. pp elastic scattering was measured at the ISR collider in the c.m. energy range 23 – 62 GeV. This was followed by the Fermilab fixed target pp elastic scattering measurements at c.m. energy 27 GeV. Then came p̄p elastic scattering measurements at the CERN SPS Collider in the half TeV c.m. energy range. Finally, in the mid-nineties, p̄p elastic differential cross sections were measured at the Fermilab Tevatron at c.m. energy 1.8 TeV, but in a small momentum transfer range[1)]. The Tevatron measurements have recently been extended to 1.96 TeV as reported at this Workshop[2)].

During the same period – early seventies to mid-nineties, various theoretical groups devoted enormous effort to develop models of nucleon structure based on low energy properties of the proton and neutron. This led to the Skyrmion model, MIT Bag model, Little Bag model, Topological Soliton model, Chiral Bag model, etc.[3] With the startup of LHC, predictions for pp elastic scattering at LHC based on various phenomenological models have been discussed recently by Kašpar et al.[4]

Our phenomenological investigation of pp and $\bar{p}$p elastic scattering began in late seventies and has now continued for three decades. From our work, we have arrived at the following physical picture of the proton. The proton appears to have three regions: an outer region of quark-antiquark ($q\bar{q}$) condensed ground state, an inner shell of baryonic charge – where the baryonic charge is geometrical or topological in nature (similar to the 'Skyrmion Model' of the nucleon) and a core region of size 0.2 fm – where valence quarks are confined. The part of the proton structure comprised of a topological baryonic charge shell and three valence quarks in a small core has been known as a chiral bag model of the nucleon in low energy studies[3]. What we are finding from high energy elastic scattering then is that – the proton is a 'Condensate Enclosed Chiral Bag'.[1]

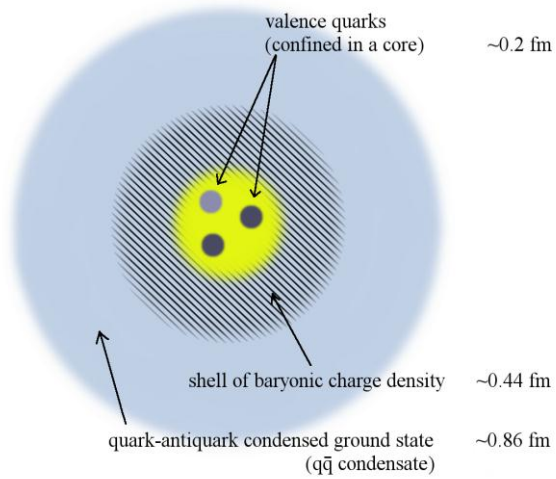

Fig.1. Physical picture of the proton – a Condensate Enclosed Chiral Bag.

2. Theoretical Development

Theoretical development of our model begins with the classic Gell-Mann-Levy linear σ-model[5] given by the following Lagrangian density:

$$\mathcal{L} = \bar{\psi}\, i\, \gamma^\mu \partial_\mu \psi + \tfrac{1}{2}\left(\partial_\mu \sigma\, \partial^\mu \sigma + \partial_\mu \vec{\pi}\, \partial^\mu \vec{\pi}\right) - G\bar{\psi}[\sigma + i\, \vec{\tau} \cdot \vec{\pi}\, \gamma^5]\psi - \lambda(\sigma^2 + \vec{\pi}^2 - f_\pi^2)^2. \qquad (1)$$

We introduce a scalar-isoscalar field $\zeta(x)$ and a unitary field $U(x)$ in the following way:

$$\sigma(x) + i\, \vec{\tau} \cdot \vec{\pi}(x) = \zeta(x) U(x), \qquad (2)$$

$\zeta(x)$ is the magnitude of the fields $\sigma(x)$ and $\vec{\pi}(x)$: $\zeta(x) = \sqrt{\sigma^2(x) + \vec{\pi}^2(x)}$. Using right and left fermion fields: $\psi_{\mathrm{R}}(x) = \frac{1}{2}(1 + \gamma^5)\, \psi(x)$, $\psi_{\mathrm{L}}(x) = \frac{1}{2}(1 - \gamma^5)\, \psi(x)$, the Lagrangian density (Eq. (1)) can now be written as:

$$\mathcal{L} = \bar{\psi}_{\mathrm{R}}\, i\, \gamma_\mu\, \partial_\mu \psi_{\mathrm{R}} + \bar{\psi}_{\mathrm{L}}\, i\, \gamma^\mu\, \partial_\mu \psi_{\mathrm{L}} + \tfrac{1}{2}\partial_\mu \zeta\, \partial^\mu \zeta + \tfrac{1}{4}\zeta^2 tr\left[\partial_\mu U\, \partial^\mu U^\dagger\right]$$
$$- G\, \zeta\, [\bar{\psi}_{\mathrm{L}} U\, \psi_{\mathrm{R}} + \bar{\psi}_{\mathrm{R}}\, U^\dagger\, \psi_{\mathrm{L}}] - \lambda(\zeta^2 - f_\pi^2)^2\,. \qquad (3)$$

In the Gell-Mann-Levy linear σ-model the pion field $\vec{\varphi}(x)$ appears through the unitary field $U(x)$: $U(x) = \exp[i\, \vec{\tau}\, \cdot \frac{\vec{\varphi}(x)}{f_\pi}]$ ($f_\pi \simeq 93$ MeV). When the scalar field $\zeta(x)$ is replaced by its ground state value f_π, the model becomes the nonlinear σ-model. The fermion fields here correspond to u, d quarks, and we are starting with a two flavor model.

The next step is to gauge this model following Bando et al. and Meissner et al. – by introducing the idea of hidden gauge symmetry. This leads to bringing in a gauge field $\mathcal{V}_\mu(x)$,

which is given by the vector mesons $\vec{\rho}$ and ω: $\mathcal{V}_\mu = -\frac{i}{2} g[\vec{\tau}\cdot\vec{\rho}_\mu + \omega_\mu]$. $\mathcal{V}_\mu(x)$ leads to a left gauge field $A_\mu^L(x)$ and a right gauge field $A_\mu^R(x)$ and the Lagrangian in the quark sector can now be written as

$$\mathcal{L}_{\rm q} = \bar{\psi}_{\rm L}\, i\,\gamma^\mu\big(\partial_\mu + A_\mu^{\rm L}\big)\psi_{\rm L} + \bar{\psi}_{\rm R}(x)\, i\,\gamma^\mu\big(\partial_\mu + A_\mu^{\rm R}\big)\psi_{\rm R} - G\,\zeta\,[\bar{\psi}_{\rm L}\, U\,\psi_{\rm R} + \bar{\psi}_{\rm R}\, U^\dagger\,\psi_{\rm L}]. \tag{4}$$

We now develop the model further by introducing quarks of three flavors u, d, s and by writing the whole model in path integral formalism. This leads to new features. The fermion measure is found to be gauge dependent. The gauge dependent fermion measure can be written in terms of gauge independent fermion measure and a Jacobian which we write as $\exp(i\,\Gamma[U,\mathcal{V}])$:

$$\int d\psi\;\; d\psi^\dagger = e^{i\,\Gamma[U,\mathcal{V}]}\int\, d\psi^0\, d\psi^{0\,\dagger} \tag{5}$$

$\Gamma[U,\mathcal{V}]$ can be identified as a new piece of action – known as Wess-Zumino-Witten (WZW) action. The action functional of the model, i.e., the whole model, can now be written as

$$e^{i\,W[U,\zeta,\mathcal{V},\psi,\psi^\dagger]} = \frac{1}{\mathcal{N}}\int dU\, d\zeta\, d\psi^0\, d\psi^{0^\dagger}\;\cdot\; e^{i\,\Gamma_{WZW}[U,\mathcal{V}]+i\,S[U,\zeta,\mathcal{V}]+i\,S[\zeta,\psi^0,\psi^{0^\dagger},\mathcal{V}]}, \tag{6}$$

where

$$S[U,\zeta,\mathcal{V}] = \int d^4x\,\mathcal{L}_U(U,\zeta,\mathcal{V}), \tag{7}$$

$$S\left[\zeta,\psi^0,\psi^{0^\dagger},\mathcal{V}\right] = \int d^4x\,[\bar{\psi}^0\;\, i\,\gamma^\mu\big(\partial_\mu + \mathcal{V}_\mu\big)\psi^0\; + \frac{1}{2}\,\partial_\mu\zeta\,\partial^\mu\zeta - G\,\zeta\,\bar{\psi}^0\psi^0 - \lambda(\zeta^2 - f_\pi^2)^2]. \tag{8}$$

We notice that all pion interactions, which enter through the unitary field $U(x)$, are contained in the action $\Gamma_{WZW}[U,\mathcal{V}]$ and $S[U,\zeta,\mathcal{V}]$, while the interaction between the scalar field and fermion fields are included in the action $S\left[\zeta,\psi^0,\psi^{0^\dagger},\mathcal{V}\right]$.

At this point, if we make the approximation $\zeta(x) = f_\pi$ in the pion sector (unitary field sector), then the model breaks up into two parts:

$$e^{iW[U,\zeta,\mathcal{V},\psi,\psi^\dagger]} \simeq \frac{1}{\mathcal{N}}\int dU\, e^{i\Gamma_{WZW}[U,\mathcal{V}]+iS[U,f_\pi,\mathcal{V}]}\int d\zeta\, d\psi^0\, d\psi^{0^\dagger} e^{iS[\zeta,\psi^0,\psi^{0^\dagger},\mathcal{V}]}. \tag{9}$$

Considering only the part with the action $\Gamma_{WZW}[U,\mathcal{V}] + S[U,f_\pi,\mathcal{V}]$ and dropping the scalar field then leads to the nonlinear σ-model (NLσM). It is this later model that describes the topological soliton model of the nucleon.

We note that the Wess-Zumino-Witten action in its simplest approximation is given by $\Gamma_{WZW}[U,\mathcal{V}] = \int d^4x\,\mathcal{L}_{WZW}$, where $\mathcal{L}_{WZW} = g_\omega\omega_\mu B^\mu$ and

$$B^\mu = \frac{1}{24\pi^2}\epsilon^{\mu\nu\rho\sigma}\, tr[U^\dagger\,\partial_\nu U\, U^\dagger\partial_\rho U U^\dagger\partial_\sigma U]. \tag{10}$$

Γ_{WZW} shows that the vector meson ω couples to the baryonic current in the same way as the photon couples to the electromagnetic current except that the baryonic current is topological, i.e., geometrical in origin. The topological soliton model has been very successful in describing the low energy properties of the nucleon except in one respect. It consistently leads to a large mass of the soliton ~1500 MeV[6)] compared to the nucleon mass 939 MeV. This has remained a major shortcoming of the topological soliton model.

3. Emergence of the Proton Structure

We notice that if we consider the scalar field in Eq. (9) as nonvanishing, then it provides an interaction between quarks and antiquarks: Eq. (8). This interaction can significantly lower the total

energy of the system compared to the case without the scalar field. We find the energy difference between having the scalar field and not having it is[7)]

$$\Delta E = \int d^3x \left[-\frac{1}{2}\left(\vec{\nabla}\zeta\right)^2 + v(\zeta) + 4\,\lambda\,\zeta^2\left({f_\pi}^2 - \zeta^2\right)\right] + E_{\mathrm{g}}^{KE}, \tag{11}$$

where $v(\zeta) = \lambda\,(\zeta^2 - f_\pi^2)^2$. If $\zeta(r)$ falls sharply from its value $\zeta(r) = f_\pi$ to $\zeta(r) = 0$ at some critical distance r_c from the origin, then the term $-\frac{1}{2}\int d^3x\left(\vec{\nabla}\zeta\right)^2$ will be very large and negative. In fact, if we take the ζ-field to be $f_\pi\,\theta(r - r_{\mathrm{c}})$, we find surface energy $-\frac{1}{2}\,f_\pi^2\,4\,\pi\,r_{\mathrm{c}}^2\,\delta(0)$ (infinitely negative). Therefore with a $\zeta(r)$ falling sharply, the mass of the soliton can easily be reduced by as much as ~600 MeV. This resolves a major problem of the topological soliton model.

However, there is an important implication of this behavior of the scalar field. If the scalar field provides the baryonic charge only in the region $r_c < r \lesssim r_B$ where $\zeta(r) = f_\pi$ (r_B: radius of the baryonic charge density), then how do we obtain total baryonic charge of one? This implies that there have to be valence quarks in the region $0 \le r \le r_c$ to make up the total baryonic charge of one.[8)] Essentially, we end up with a chiral bag as nucleon structure.[3)]

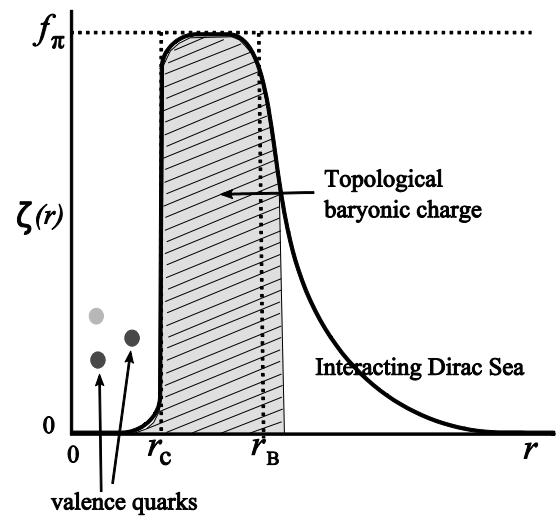

Fig. 2. The scalar field $\zeta(r)$ as a function of r. r_{C}: radius of the core, r_B: radius of the baryonic charge density.

Next we ask the question: what is the behavior of the scalar field $\zeta(r)$ in the region $r > r_B$? We envisage a behavior as shown in Fig. 2 indicating that $\zeta(r)$ decreases smoothly to zero. The nonvanishing scalar field in the region $r > r_B$ makes the quarks and antiquarks in the Dirac sea massive. This lowers the energy of the Dirac sea compared to the noninteracting Dirac sea, which is the normal vacuum. We then have a condensed $q\bar{q}$ ground state surrounding the chiral bag structure,[8)] and we end up with the proton structure shown in Fig. 1.

4. Elastic Scattering Processes

Given the structure of the proton that has emerged from our theoretical investigation, we envision three main processes giving rise to pp elastic scattering (Fig. 3):

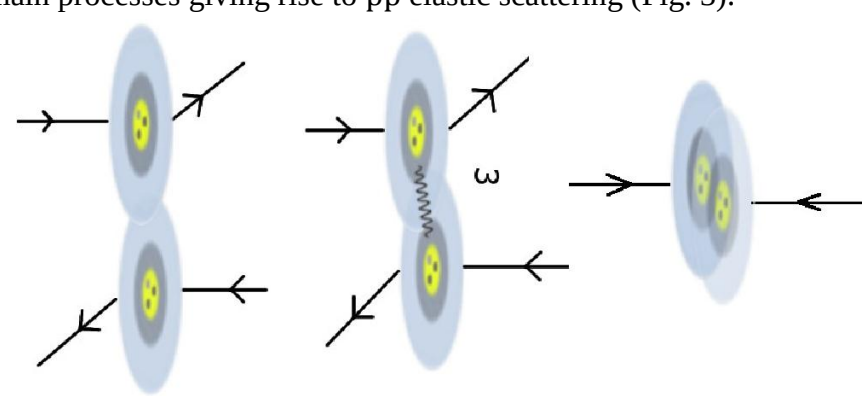

diffraction ω-exchange short-distance collision ($b \lesssim 0.1$ fm)

Fig. 3. Elastic scattering processes.

i) in the small $|t|$region, the outer cloud of one proton interacts with that of the other giving rise to diffraction scattering; ii) in the intermediate $|t|$ region, the baryonic charge of a proton probes that of the other via ω-exchange; iii) in the large $|t|$ region, i.e., short-distance collision ($b \lesssim 0.1$ fm) – a valence quark from one proton scatters off a valence quark from the other proton (as shown in Fig. 4).

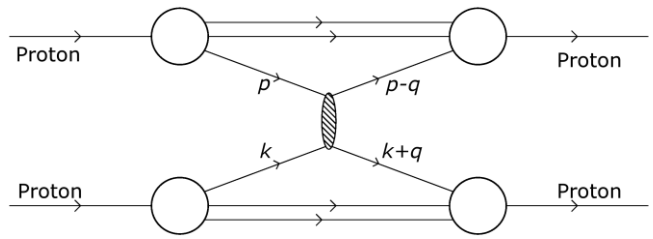

Fig.4. Hard collision of a valence quark from one proton with one from the other proton.

We have considered two QCD processes for the quark-quark scattering (Fig. 5): (a) exchange of gluons in the form of gluon ladders (hard pomeron exchange); (b) low-x gluon cloud of one quark interacting with that of the other.

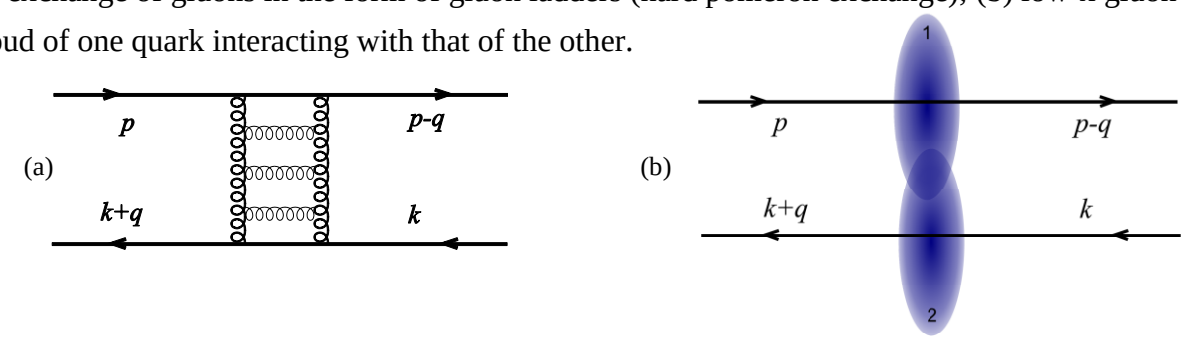

Fig. 5. QCD processes for valence quark-quark scattering.

How elastic scattering amplitudes due to diffraction, ω-exchange, hard pomeron exchange, and low-x gluon cloud-cloud interaction are calculated has been presented by us earlier[9]. The diffraction amplitude has the following important asymptotic properties:

1. $\sigma_{tot}(s) \sim (a_0 + a_1 \ln s)^2$ (Froissart – Martin bound)

2. $\rho(s) \simeq \frac{\pi\, a_1}{a_0 + a_1 \ln s}$ (derivative dispersion relation)

3. $T_D(s,t) \sim i\, s \ln^2 s\, f(|t|\ \ln^2 s)$ (Auberson-Kinoshita-Martin scaling)

4. $T_D^{\bar{p}p}(s,t) = T_D^{pp}(s,t)$ (crossing even)

5. Comparison with TOTEM Results

We now show our $d\sigma/dt$ prediction (solid line) at $\sqrt{s}$ = 7 TeV together with the TOTEM Collaboration measurements at LHC (Fig. 6). The blue dashed line represents the first set of TOTEM results and the red dashed line represents their second

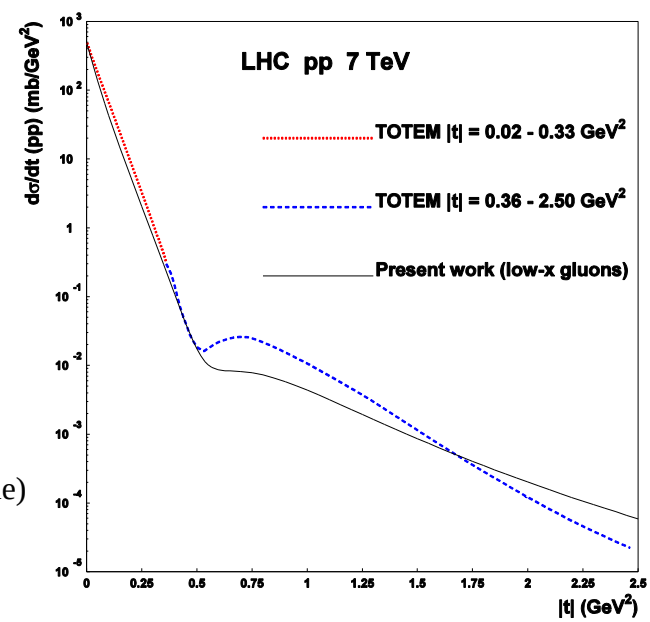

Fig.6. Comparison of our $d\sigma/dt$ prediction at $\sqrt{s}$ = 7 TeV with the TOTEM Collaboration measurements at LHC.

set.[10] We notice that our prediction of $d\sigma/dt$ in the small $|t|$ region: $|t| = 0.02 - 0.33, 0.36 - 0.47$ GeV^2 agrees quite well with the TOTEM $d\sigma/dt$ measurements. On the other hand, our $d\sigma/dt$ prediction in the momentum transfer region $|t| \simeq 0.5 - 2.5$ GeV^2 disagrees significantly with the TOTEM results. We attribute this as originating from multiple ω-exchanges at LHC at c.m. energy 7 TeV as opposed to single ω-exchange that we assumed – based on ISR data of c.m. energy ~ 50 GeV.

Table 1. Comparison with TOTEM results.

$\sqrt{s}$ = **7 TeV**	Our results	TOTEM
σ_{tot}	97.5 mb	98.3 ± 3.0 mb
σ_{el}	19.8 mb	24.8 ± 1.4 mb
$\rho(t=0)$	0.127	–
$B(t=0)$	27.77 GeV^{-2}	20.1 ± 0.5 GeV^{-2}
$\frac{d\sigma}{dt}(t=0)$	493.4 mb/GeV^2	503.7 ± 28.2 mb/GeV^2

We also present a number of our calculated results compared with the TOTEM results in Table 1.

6. Closing Comments

1. From our point of view, LHC and TOTEM have found evidence of the outer cloud of the proton. The reason is that our prediction for diffraction scattering, which originates from the cloud-cloud interaction, agrees quite well with the differential cross sections measured by the TOTEM Collaboration in the small $|t|$ region.

2. The low energy nucleon models have led us to surmise correctly the chiral bag part of the proton structure.

3. We attribute the disagreement of our $d\sigma/dt$ prediction with TOTEM measurements in the region $|t| \sim 0.5 - 2.5$ GeV^2 as due to multiple ω-exchanges at LHC instead of a single ω-exchange that we assumed.

4. Our investigation has shown that a single effective field theory model can describe the proton structure that we have arrived at.

References

1. M. M. Islam, J. Kašpar, R. J. Luddy, A. V. Prokudin, *CERN Courier*, December 2009, p.35.
2. DØ Results on Diffraction, C. Royon, CEA Saclay, France.
3. A. Hosaka and H. Toki, Quarks, Baryons and Chiral Symmetry (World Scientific), 2001.
4. J. Kašpar, V. Kundrát, M. Lokajíček, J. Procházka, *Nucl. Phys.* **B 843** (2011) 84.
5. M. M. Islam, R. J. Luddy and A. V. Prokudin, *Int. J. Mod. Phys*. **A21** (2006) 1-41.
6. L. Zhang and N. C. Mukhopadhyay, *Phys. Rev.* **D50** (1994) 4668.
7. M. M. Islam, *Z. Phys.* **C53** (1992) 253.
8. M.M.Islam, J.Kašpar and R.J.Luddy, Proceedings of the 11th Workshop on Non-Perturbative QCD, Paris 2011, edited by B.Mueller, M.A.Rotondo and C-I.Tan: http://www.slac.stanford.edu/econf/C1106064/papers/Islam.pdf
9. M. M. Islam, J. Kašpar, R. J. Luddy and A. V. Prokudin, *Proceedings of the 13th Int. Conf. on Elastic and Diffractive Scattering* (EDS 2009, CERN), edited by M. Deile, D. d'Enterria and A. De Roeck, p.48.
10. The TOTEM Collaboration, G. Antchev et al., *EPL*, **95** (2011) 41001; *EPL*, **96** (2011) 21002.